EFFICIENCY OF Al AND Cu ADDITION IN ZnO SORBENTS FOR DESULFURIZATION

Amphon Nitthaisong[1], Sumittra Charojrochkul[2], and Sutin Kuharuangrong[1,*]

Received: April 11, 2016; Revised: July 15, 2016; Accepted: July 27, 2016

Abstract

ZnO with a 20 mol%Al (ZA20) or 20 mol%Cu (ZC20) addition synthesized by the citrate-gel method were compared for desulfurization efficiency, particularly H_2S, at 300°C. The XRD results show the solid solution between the $ZnAl_2O_4$ and ZnO phases in ZA20 while 2 phases of hexagonal ZnO and monoclinic CuO appear in ZC20. The surface area increases in ZA20 but decreases in ZC20 as compared to ZnO. The desulfurization performance via a fixed-bed reactor shows ZC20 has a higher sulfur sorption capacity than ZA20 and ZnO, respectively. The products after desulfurization characterized by XRD are ZnS and ZnO in ZA20 while ZnS and CuS exist in ZC20. SEM micrographs show the larger grain sizes after desulfurization for all samples.

Keywords: Desulfurization, ZnO, H_2S, citrate gel method

Introduction

Zinc oxide (ZnO) has been widely used as a catalyst and an absorbent (Moezzi *et al.*, 2012). Other absorbents such as CuO/SBA-15 (Karvan and Atakül, 2008), Fe-based (Xie *et al.*, 2010), Zn-Al based and Zn-Ti based absorbents (Jung *et al.*, 2006), have been studied for desulfurization. CuO/SBA-15 increased the breakthrough sulfur capacity with the Cu content after the third desulfurization cycle at 500°C (Karvan and Atakül, 2008). Fe-based sorbents showed a longer breakthrough time with a higher desulfurization temperature from 420°C to 620°C (Xie *et al.*, 2010) while the breakthrough time of Zn-Al based and Zn-Ti based sorbents increased with a higher surface area and pore volume after desulfurization at 480°C (Jung *et al.*, 2006). The oxides of Zn, Cu, Fe, Mn, Co, and Ce supported on γ-Al_2O_3 were investigated for desulfurization in the

---

[1] *School of Ceramic Engineering, Institute of Engineering, Suranaree University of Technology, Nakhon Ratchasima, 30000, Thailand. Tel. 0 4422 4474; E-mail: sutin@sut.ac.th*

[2] *National Metal and Materials Technology Center, Pathum Thani, 12120, Thailand.*

[*] *Corresponding author*

temperature range of 500-700°C (Ko *et al.*, 2005). Among these, Mn/γ-Al_2O_3 exhibited the highest sulfur capacity after desulfurization. However, ZnO is the most attractive absorbent material due to its high sulfur sorption capacity and its breakthrough performance depends on the dopants (Garces *et al.*, 2010, Yang and Tatarchuk, 2010). During desulfurization, ZnO reacts with H_2S to produce ZnS and water, as follows (Wang *et al.*, 2008):

$$ZnO + H_2S \rightarrow ZnS + H_2O \qquad (1)$$

Cu-doped ZnO on highly porous SiO_2 support materials was investigated and demonstrated its superior desulfurization performance at the temperature range from 250°C to 400°C due to increasing oxygen vacancies from the charge compensation of Cu^{+1} substituted into ZnO (Yang and Tatarchuk, 2010). Al-doped ZnO prepared from nanoparticles was reported to improve the H_2S absorption rate due to the excess charge of Al breaking the H_2S bond (Parhoodeh *et al.*, 2012). Kang *et al.* (2007) prepared their sorbents from Cu, Zn, and Al nitrates by the co-precipitation method. They found that the CuO/ZnO (Cu:Zn = 1:1 mole ratio) and CuO/ZnO/Al_2O_3 (Cu:Zn:Al = 1:1:0.15) sorbents exhibited higher sulfur removal capacities as compared with the commercial ZnO, ZnO/Al_2O_3 (Zn:Al = 1:0.15 mole ratio) and CuO/Al_2O_3 (Cu:Al = 1:0.15 mole ratio) sorbents. Barroso *et al.* (2006) prepared CuZnAl catalysts by the citrate sol-gel method and calcined them at 500°C and 700°C. The final phases of samples with a Cu loading higher than 8 wt% were $ZnAl_2O_4$ and CuO after calcination at 500°C. In addition, the X-ray diffractometer (XRD) patterns of the ZnO and Al_2O_3 phases were no longer detected. For a higher temperature at 700°C, the diffraction patterns of $ZnAl_2O_4$ were significantly more intense while the excess of Zn formed the ZnO phase. However, the desulfurization has not been reported in this publication.

The efficiency of sulfur absorption depends on not only the atomic type addition but also on the surface area of the sorbent. In this work, CuO and Al_2O_3 additions in ZnO sorbents were synthesized by the citrate- gel method for gas desulfurization, particularly H_2S from simulated biogas. The effect of Cu and Al on the desulfurization performance will be investigated at 300°C. In addition, the microstructure from a scanning electron microscope (SEM) and the surface area from the Brunauer-Emmett-Teller (BET) method will be studied and related to the breakthrough capacity of these materials.

Meterials and Methods

The sorbents were synthesized by the citrate-gel method from zinc nitrate hexahydrate ($Zn(NO_3)_2 \cdot 6H_2O$, 98% purity), aluminum nitrate nonahydrate ($Al(NO_3)_3 \cdot 9H_2O$, 98% purity), and copper nitrate hemi-pentahydrate ($Cu(NO_3)_2 \cdot 2.5H_2O$, 98% purity) as starting materials. They were dissolved in 50 mL of deionized water with the total metal concentration of 1.0 mol/L at a mole ratio of Zn:(l or Cu) = 1:0 (ZnO), Zn:Al = 0.8:0.2 (ZA20), and Zn:Cu = 0.8:0.2 (ZC20). The citric acid ($C_6H_8O_7 \cdot H_2O$, 99.99% purity) solution was added into the nitrate solution as the polymerizable combustion fuel and stirred with a magnetic stirrer. The mole ratio of the metal ion and citric acid was 1:1.5. During mixing, the mixed solution was heated to 100°C on a hot plate. When the water evaporated, the solution became viscous and changed to gel. During continuous heating to 200°C, the gel slowly foamed, bloated, and finally changed to be a residue. The residue powders were ground and mixed with polyvinyl alcohol as a binder and glutinous rice flour to shape stability. The mixed powders were extruded in a cylindrical shape with a diameter of 2 mm and 1 cm in length. After drying, all samples were fired at 600°C and held at the reaction temperatures to burn out the binder.

The component phases of the samples were characterized by means of X-ray diffraction using a D2 PHASER diffractometer (Bruker Corp., Billerica, MA, USA) with CuK_α radiation in the 2θ range of 25°-70° with a step size of 0.02°. The quantitative phase analysis of sorbents was performed by the Rietveld method using the TOPAS 4.2 software. The Rietveld refinements were performed using the structural database of the Crystallography Open Database.

The microstructures of the calcined sorbents were recorded on the fracture surface by using a Quanta 450 SEM (FEI Company, Hillsboro, OR, USA). The specific surface area of the sorbents was investigated by the BET method using an ASAP 2010 instrument (Micrometrics Instrument Corp., Norcross, GA, USA). Degassed pre-treatments were operated at 200°C under vacuum for 6 h. The BET surface area and pore volume were analyzed by adsorption of N_2 at -196°C on 0.2 g of the fresh sorbents.

The desulfurization performance for all samples was measured at 300°C with an experimental setup, as shown in Figure 1. From the sorbent, 0.1 g was placed in the vertical fixed-bed tubular reactor made from borosilicate glass with an internal diameter of 0.65 cm and supported by quartz wool. The sorbents were heated to the operating temperature with flowing N_2 at 10 ml/min and held at this temperature for 1 h before flowing a certified mixed gas (H_2S: 0.3629%, CO_2: 20.07%, CH_4: 74.88% and N_2: Balance) as a simulated biogas to the reactor. The gas flow rate was controlled at 10 ml/min by using a SmartTrak® 2: 100 Series model C100L-DD-2-ON1-SK1-PV2-V1-S0-GS mass flow controller (Sierra Instruments, Inc., Monterey, CA, USA). The outlet gas was analyzed by a Varian 490-GC Micro gas chromatograph (Agilent Technologies, Inc., Santa Clara, CA, USA) equipped with a 10 m PoraPlot U column and a thermal conductivity detector. The sulfur sorption capacity was determined by the breakthrough time defined at 3% of H_2S concentrations at the outlet. After desulfurization, the component phases and their amounts of sorbents were characterized using an XRD with the same condition as previously mentioned.

Results and Discussion

The XRD patterns of the fresh sorbents for all samples are shown in Figure 2. The result for ZnO shows a single phase of hexagonal ZnO correlated with the powder diffraction file (PDF) 36-1451. For ZA20, the XRD results show 2 phases of hexagonal ZnO and cubic $ZnAl_2O_4$ matched with PDF 36-1451 and 05-0669, respectively. Other phases of zinc aluminum oxide in the phase diagram between ZnO and Al_2O_3 are not matched with this pattern. In addition, ZA20 performs peak

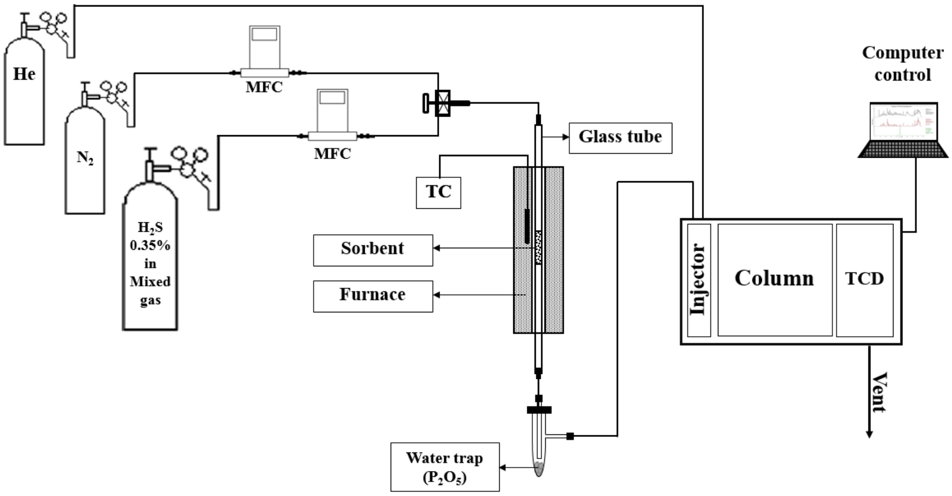

Figure 1. Schematic representation of the desulfurization experimental set up MFC: mass flow controller, TC: thermocouple, TCD: thermal conductivity detector

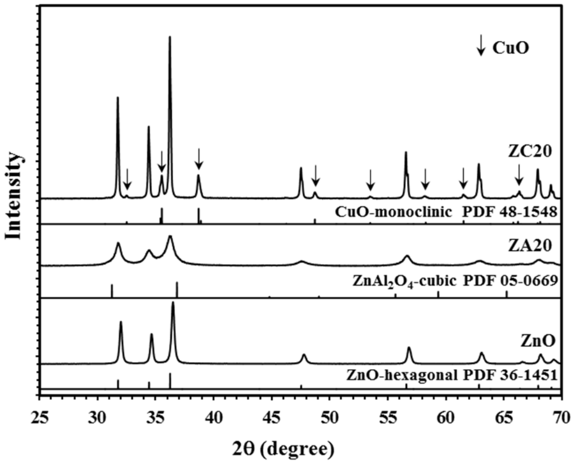

Figure 2. XRD patterns of fresh sorbents before desulfurization

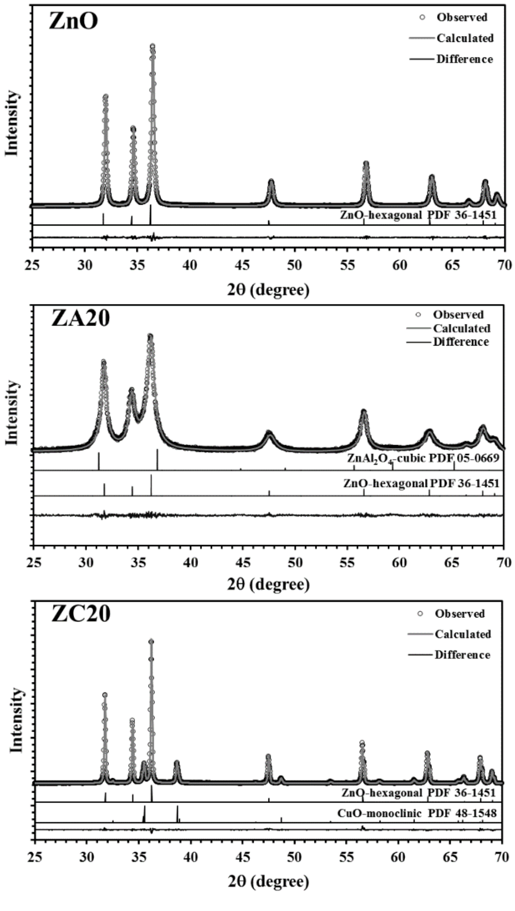

Figure 3. Rietveld plots for all fresh sorbents with the difference curve (at the bottom) between the experimental data and fitting profile

broadening, implying a formation of a solid solution between ZnO and $ZnAl_2O_4$ in this composition. For ZC20, the results show 2 phases of hexagonal ZnO and monoclinic CuO matched with PDF 36-1451 and 48-1548, respectively. The strongest peak intensities of the CuO phase can be observed at 2θ = 35.5° and 38.7° as indicated by arrows. The peaks of the ZnO and CuO phases appear at different 2θ, indicating that there is no solid solution between these 2 phases due to their different structures. The quantitative analysis and the lattice parameters of all specimens are determined from the XRD patterns using the Rietveld refinement method. Figure 3 shows the results of the experimental data and calculated patterns including the difference between these 2 as indicated at the bottom. The weight fractions of each phase including lattice parameters for all compositions are summarized in Table 1. R_{wp} represents the overall weighted-profile R-value and R_{exp} is the expected R-value. These 2 factors are defined as (Snellings *et al.*, 2010):

$$R_{wp} = \sqrt{\frac{\sum w_i (I_{i_{obs}} - I_{i_{cal}})^2}{\sum w_i I_{i_{obs}}^2}} \tag{2}$$

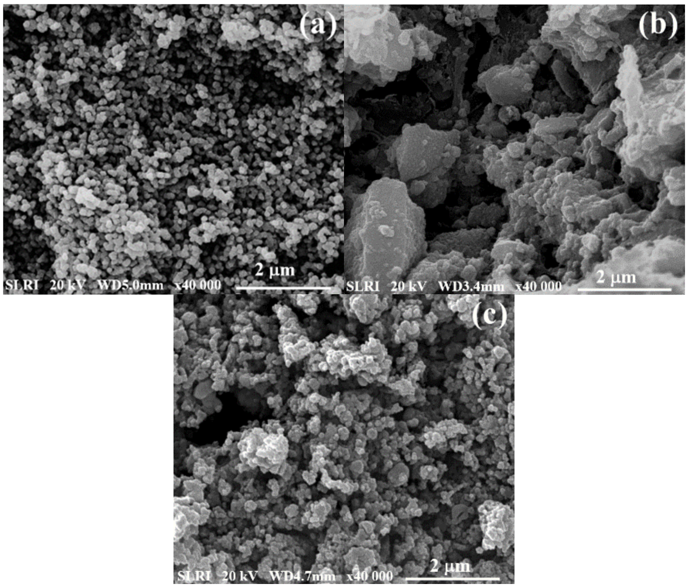

Figure 4. SEM micrographs before desulfurization for (a) ZnO, (b) ZA20, and (c) ZC20

Table 1. Quantitative phase analysis for all samples before desulfurization

Sorbent	Phase	wt%	R_{wp}	R_{exp}	GoF	SG	a(Å)	b(Å)	c(Å)
ZnO			**6.64**	**5.96**	**1.11**				
	ZnO	100.00				*P63mc*	3.2494		5.2050
ZA20			5.23	4.60	1.14				
	ZnO	74.78				*P63mc*	3.2514		5.1885
	$ZnAl_2O_4$	25.22				*Fd-3m*	8.0840		
ZC20			4.67	3.78	1.23				
	ZnO	79.25				*P63mc*	3.2497		5.2046
	CuO	20.75				*C2/c*	4.6903	3.4218	5.1330

Rwp = weighted-profile R value, Rexp = expected R value, GoF = goodness of fit, SG = Space Group

$$R_{exp} = \sqrt{\frac{(N-P)}{\Sigma w_i I_{i_{obs}}^2}} \quad (3)$$

where $I_{i_{obs}}$ is the observed intensity at a certain 2θ, $I_{i_{cal}}$ is the calculated intensity at the same angle, $w_i = 1/I_{i_{obs}}$, N is the number of data points, and P is the number of refined parameters. GoF is the goodness of fit which is the ratio of R_{wp} over R_{exp}. Its value for a perfect refinement would equal 1; however, its results in this work range from 1.08-1.23, which is acceptable due to the small difference between the experimental data and fitting profile, as shown at the bottom of Figure 3.

Figure 4(a-c) shows the SEM images before desulfurization for ZnO, ZA20, and ZC20, respectively. The ZnO and ZC20 specimens show a porous structure with small grains and the average grain size of all compositions determined from the line intercept method is in a range of 48 – 160 nm. However, ZA20 shows an agglomeration of small grains.

Table 2 shows the surface area and pore volume of all specimens determined from the BET method. The result shows that the surface area and pore volume increased with the 20 mol%Al addition as compared to those of ZnO. On the other hand, the surface area and pore volume slightly decrease with the 20 mol%Cu addition. This suggests that ZA20 has a smaller grain size than ZnO and ZC20. Figure 5 shows the breakthrough curves of all sorbents after desulfurization at 300°C. The breakthrough time is determined at 3%H_2S concentrations detected at the outlet and the breakthrough time of 8.62 min without the sorbent is used for calibration. From the results, the ZnO sorbents reach the breakthrough line at 3%H_2S concentrations in 14 min. The breakthrough time for ZA20 and ZC20 increases and ZC20 shows the highest breakthrough time at 526 min. The breakthrough capacity can be determined from the following equation (Wang, 2008):

$$\text{Breakthrough capacity} = \frac{V_{H_2S} \times t_b \times C_{in} \times MW_{Sulfur}}{W_{sorbent}} \quad (4)$$

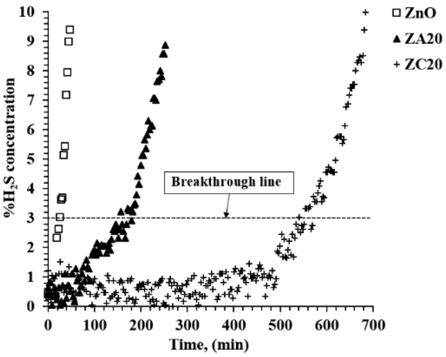

Figure 5. Breakthrough curves of all sorbents after desulfurization at 300°C

Table 2. BET surface area and total pore volume before desulfurization and the breakthrough performance at 300°C for all sorbents

Sorbent	S_{BET} (m^2/g)	P_V (cm^3/g)	Breakthrough time (min)	Breakthrough capacity	
				(g S/g Sorb)	(mol/g Sorb)
ZnO	8.15	4.69x10^{-2}	14	0.16	4.86x10^{-3}
ZA20	65.99	14.0x10^{-2}	131	1.43	4.46x10^{-2}
ZC20	7.40	2.3x10^{-2}	526	5.95	1.86x10^{-1}

S_{BET} = BET surface area, P_V = Total pore volume.

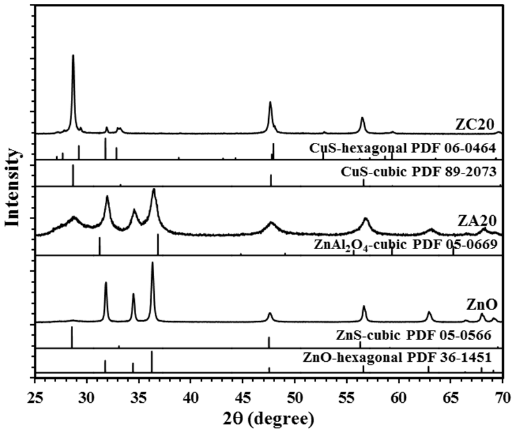

Figure 6. XRD patterns of all sorbents after desulfurization at 300°C

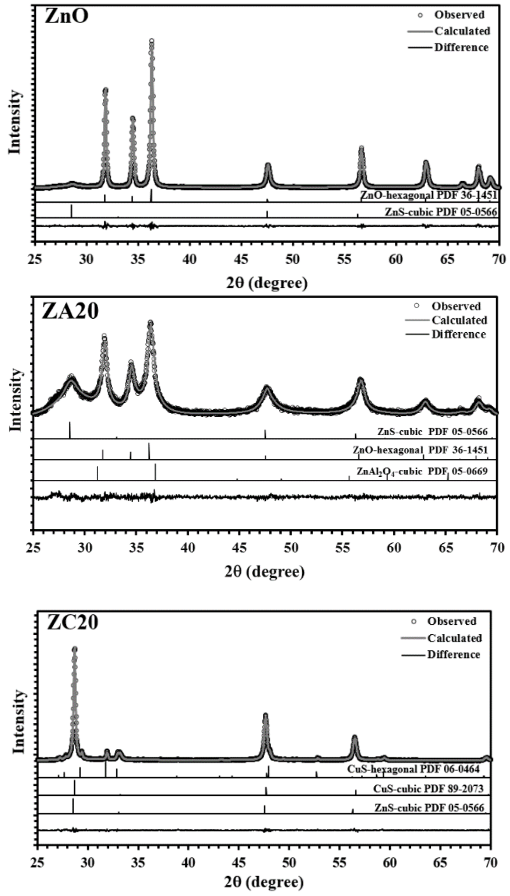

Figure 7. Rietveld plots for all sorbents after desulfurization at 300°C with the difference curve (at the bottom) between the experimental data and fitting profile

where V_{H_2S} is the volumetric rate of feed gas (10 ml/min), t_b is the breakthrough time in min, C_{in} is the inlet H_2S concentration ($0.3629\text{x}10^{-5}$ mol/ml), MW_{Sulfur} is the molecular weight of element sulfur (32.066 g/mol), and $W_{sorbent}$ is the sorbent loading in the reactor in g. The breakthrough performances after desulfurization for all sorbents are summarized in Table 2. From the results, ZC20 having less surface area and pore volume achieves a higher breakthrough capacity than ZnO and ZA20. This result indicates that the type of atom addition in ZnO performs more effective desulfurization than the surface area of the sorbents.

Figure 6 shows the XRD patterns of all sorbents after desulfurization at 300°C. For ZnO, a small hump at $2\theta = 28.5°$ appears with the ZnO main phase and can be indexed as a cubic ZnS (PDF 05-0566). This result implies that ZnO can absorb a small amount of sulfur from H_2S and transform to ZnS. For ZA20, the peak intensity at $2\theta = 28.7°$ matched with a cubic ZnS can be observed, although the diffraction peaks of ZnO and $ZnAl_2O_4$ still remain in ZA20 similar to those before desulfurization. The weight fraction of $ZnAl_2O_4$ from the Rietveld refinement in Table 3 does not change after desulfurization as compared to that in Table 1. Nevertheless, the amount of ZnO decreases, suggesting that ZnS amount of ZnO decreases, suggesting that ZnS forms from ZnO, not $ZnAl_2O_4$. The results from ZC20 show the strongest intensity at $2\theta = 28.6°$ matched with either the ZnS cubic (PDF 05-0566) or CuS cubic phases (PDF 89-2073). Both of them have a similar structure and lattice parameter as given in Table 3, thus there is probably the formation of a solid solution between these 2 compounds. Furthermore, there are other peaks observed at $2\theta = 31.8°$ and 32.8° that can be indexed as hexagonal CuS (PDF 06-0464). The strongest peaks of ZnO at $2\theta = 36.3°$ and CuO at $2\theta = 35.5°$ and 38.7° disappear after desulfurization, with the result that all of the ZnO and CuO in ZC20 can

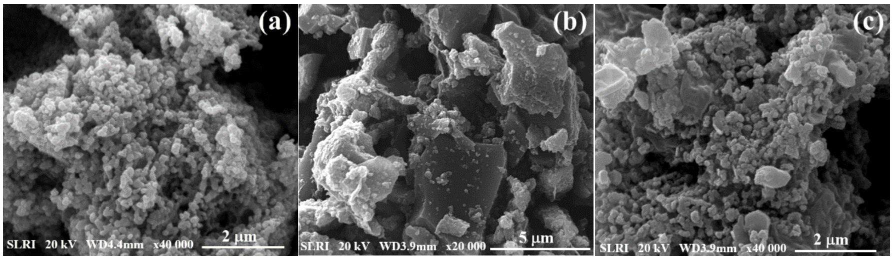

Figure 8. SEM micrographs after desulfurization at 300°C for (a) ZnO, (b) ZA20, and (c) ZC20

Table 3. Quantitative phase analysis for all sorbents after desulfurization at 300°C

Sorbent	Phase	wt%	R_{wp}	R_{exp}	GoF	SG	a(Å)	b(Å)	c(Å)
ZnO			7.47	6.76	1.11				
	ZnO	97.28				*P63mc*	3.2493		5.2050
	ZnS	2.72				*F-43m*	5.4000		
ZA20			7.24	6.70	1.08				
	ZnO	60.31				*P63mc*	3.2400		5.1990
	ZnS	14.49				*F-43m*	5.4000		
	$ZnAl_2O_4$	25.20				*Fd-3m*	8.0846		
ZC20			7.14	6.01	1.19				
	ZnS	80.30				*F-43m*	5.4000		
	CuS	3.63				*F-43m*	5.4017		
	CuS	16.07				*P63/mmc*	3.7866		16.3262

R_{wp} = weighted-profile R value, R_{exp} = expected R value, GoF = goodness of fit, SG = Space Group absorb sulfur from H_2S. This suggests that ZC20 can completely absorb sulfur and transform from oxide to sulfide compounds at 300°C.

Figure 8(a-c) shows the SEM images of all specimens after desulfurization at 300°C. The particles of new sulfides for ZA20 and ZC20 are larger than those of oxides before desulfurization due to the larger lattice parameters of ZnS and CuS. This confirms the results from the XRD after desulfurization.

Conclusions

ZnO and 20 mol%Al or 20 mol%Cu additions into ZnO have been synthesized by the citrate gel method and calcined at 600°C. ZnO and $ZnAl_2O_4$ form a solid solution in ZA20 but the phases of hexagonal ZnO and monoclinic CuO separately appear in ZC20 due to the different crystal structure. Although ZA20 has a higher surface area than ZC20, the breakthrough capacity at 300°C is less than that of ZC20. All of the ZnO and CuO in ZC20 transform to ZnS and CuS but only small amounts of ZnO in the ZnO and ZA20 sorbents can absorb sulfur from H_2S. After desulfurization, the larger particles are obtained from sulfide compounds in ZA20 and ZC20.

Acknowledgements

All chemicals and the desulfurization testing system in this work were supported by Materials for Energy Research Unit, National Metal and Materials Technology Center (MTEC), Thailand

References

Barroso, M.N., Gomez, M.F., Gamboa, J.A., Arrua, L.A., and Abello, M.C. (2006). Preparation and characterization of CuZnAl catalysts by citrate gel process. J. Phys. Chem. Solids, 67:1583-1589.

Garces, H.F., Galindo, H.M., Garces, L.J., Hunt, J., Morey, A., and Suib, S.L. (2010). Low temperature H_2S dry-desulfurization with zinc oxide. Micropor. Mesopor. Mat., 127:190-197.

Jung, S.Y., Lee, S.J., Lee, T.J., Ryu, C.K., and Kima, J.C.. (2006). H_2S removal and regeneration properties of Zn–Al-based sorbents promoted with various promoters. Catal. Today, 111:217-222.

Kang, S-H., Bae, J-W., Kim, H-T., Jun, K-W., Jeong, S-Y., and Chary, K.V.R. (2007). Effective removal of odorants in gaseous fuel for the hydrogen station using hydrodesulfurization and adsorption. Energ. Fuel., 21:3537-3540.

Karvan, O. and Ataкül, H. (2008). Investigation of CuO/mesoporous SBA-15 sorbents for hot gas desulfurization. Fuel Process. Technol., 89:908-915.

Ko, T-H., Chu, H., and Chaung, L-K. (2005). The sorption of hydrogen sulfide from hot syngas by metal oxides over supports. Chemosphere, 58:467-474.

Moezzi, A., McDonagh, A.M., and Cortie, M.B. (2012). Zinc oxide particles: Synthesis, properties and applications. Chem. Eng. J., 185-186:1-22.

Parhoodeh, S., Shoushtari, M.Z., and Farbod, M. (2012). Efficient absorption of H_2S by aluminum doped zinc oxide nanoparticles. Mater. Lett., 78:188-191.

Snellings, R., Machiels, L., Mertens, G., and Elsen, J. (2010). Rietveld refinement strategy for quantitative phase analysis of partially amorphous zeolitized tuffaceous rocks. Geol. Belg., 13(3):183-196.

Wang, D.M. (2008). Breakthrough behavior of H_2S removal with an iron oxide based CG-4 adsorbent in a fixed-bed reactor, [MSc. thesis]. Department of Chemical Engineering, College of Graduate Studies and Research, University of Saskatchewan. Saskatoon, SK, Canada, 113p.

Wang, X., Sun, T., Yang, J., Zhao, L., and Jia, J. (2008). Low-temperature H_2S removal from gas streams with SBA-15 supported ZnO nanoparticles. Chem. Eng. J., 142:48-55.

Xie, W., Chang, L., Wang, D., Xie, K., Wall, T., and Yu, J. (2010). Removal of sulfur at high temperatures using iron-based sorbents supported on fine coal ash. Fuel, 89:868-873.

Yang, H. and Tatarchuk, B. (2010). Novel-doped zinc oxide sorbents for low temperature regenerable desulfurization applications. AIChE Journal, 56:2898-2904.